Segregation-enhanced etching of Cd during Zn deposition on CdSe quantum dots

T. Passow,* H. Heinke, T. Schmidt, J. Falta, A. Stockmann, H. Selke, P. L. Ryder, K. Leonardi, and D. Hommel
Universität Bremen, Institut für Festkörperphysik, P.O. Box 330 440, 28334 Bremen, Germany
(Received 3 July 2001; published 26 October 2001)

CdSe/ZnSe quantum structures grown on GaAs(001) by molecular-beam epitaxy were systematically investigated by high-resolution x-ray diffraction and high-resolution transmission-electron microscopy. Half of the initial Cd deposit redesorbs when migration-enhanced epitaxy is used instead of conventional molecular-beam epitaxy for the overgrowth of the CdSe by ZnSe. This result is explained by a segregation model accounting for an enhanced redesorption of Cd due to Cd segregation and replacement of Cd by Zn in the topmost surface layers. The observed intermixing of CdSe/ZnSe can be explained by this model.

DOI: 10.1103/PhysRevB.64.193311 PACS number(s): 68.35.Dv, 68.35.Fx, 81.05.Dz

The system CdSe/ZnSe is in the center of interest because of its high lattice mismatch of about 7%, which is expected to result in self-assembled quantum dots during epitaxial growth[1–4] and its possible application for optoelectronic devices in the yellow/green/blue spectral range. Recently, a strong intermixing leading to broadened ternary quantum structures was reported by different groups,[5–11] but the origin of this intermixing is still under discussion. From the widely studied system InAs/GaAs, which has a similar lattice mismatch, the importance of surface segregation for intermixing is well known.[12] Surface segregation was also observed in the system CdSe/ZnSe (Refs. 5 and 10) but the rather symmetrical depth profiles of composition found by high-resolution transmission-electron microscopy (HRTEM) are commonly interpreted in terms of interdiffusion.[11] However, this results in Cd diffusion constants, which are orders of magnitude higher than those determined by annealing experiments.[9,11] In order to clarify the role of surface segregation, we have varied the method of ZnSe-cap-layer deposition under controlled conditions. Conventional molecular-beam epitaxy (MBE) and migration-enhanced epitaxy (MEE) have been used for cap-layer growth. The situation at the growing surface is changed drastically in the latter case due to alternate supply of group-II and -VI elements. The influence of the overgrowth parameters is systematically studied by high-resolution x-ray diffraction (HRXRD), grazing incidence x-ray diffraction (GIXRD), and HRTEM.

HRXRD as well as HRTEM give information about the incorporated amount of CdSe. Additionally, HRTEM provides knowledge on the depth distribution of Cd, which is hardly accessible by HRXRD due to the small scattering volume of CdSe quantum-dot structures. Structural information on extremely thin layers at the sample surface can be obtained by GIXRD despite the small scattering volume. This enables to investigate the structural properties of CdSe quantum dots *before* overgrowth by ZnSe.

The samples were grown at 280 °C on GaAs(001) substrates in a twin-chamber MBE system (EPI 930) equipped with Zn, Se, and Cd elemental sources for II-VI layer growth. The CdSe layers were deposited by MEE at 0.029 ML per second and are embedded in a 40–50-nm-thick ZnSe buffer layer and a 20–25-nm ZnSe cap layer. The intended CdSe layer thickness varies from 0.8 ML to 2.8 ML. Two different sample series were investigated, which differ in the method of the cap-layer growth. The CdSe is directly capped with ZnSe by common MBE for sample series 1 using a VI/II beam equivalent pressure ratio (BEPR) of 2:1 (i.e., stoichiometric conditions) and a growth rate of 0.5 ML/s. In contrast, the first 5 ML of ZnSe are deposited by MEE at 0.025 ML/s for sample series 2. To study the effect of the VI/II flux ratio, two samples were grown where the CdSe is overgrown by conventional MBE using a growth rate of 0.2 ML/s and a BEPR of 4:1 and 1:1, respectively. One sample with a nominal deposit of 4.9-ML CdSe and without a ZnSe cap layer was grown also for GIXRD investigations.

The HRXRD measurements were performed using a high-resolution x-ray diffractometer (Philips MRD) with a sealed Cu anode, a $4\times$Ge(220) monochromator, and a receiving slit. The GIXRD measurements were done at beamline BW1 at the Hamburg Synchrotron radiation facility (HASYLAB) employing a focused beam at a photon energy of 9.6 keV.

A Philips CM20/UT operating at 200 kV with a point resolution of 0.19 nm was used for HRTEM. The specimens were prepared by mechanical grinding followed by xenon ion milling to electron transparency.

HRXRD enables to derive very accurately the total (i.e.,

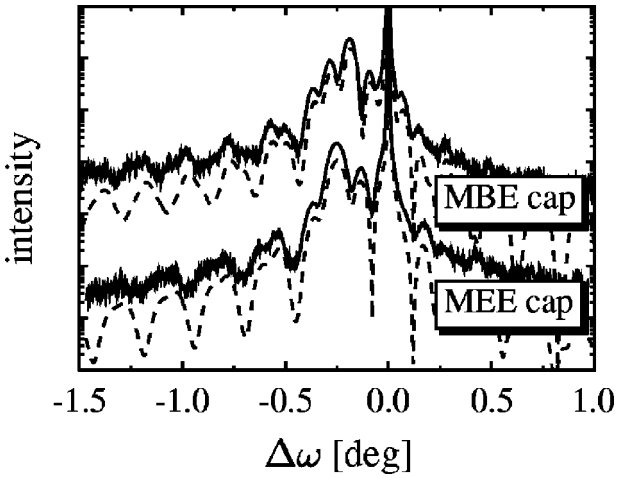

FIG. 1. Experimental (solid) and theoretical (dashed) (004) $\omega/2\theta$ scans for the samples capped by MBE (series 1) and MEE (series 2) with a CdSe deposition of 5 MEE cycles.

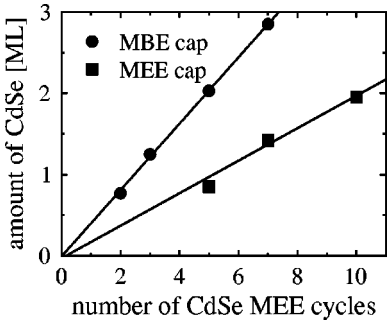

FIG. 2. Amount of CdSe determined by HRXRD vs number of CdSe MEE cycles with the ZnSe overlayer grown by MBE and MEE. The lines represent linear fits to the data.

integrated) CdSe content in the quantum structures.[7] Figure 1 shows (004) $\omega/2\theta$ scans for two samples of series 1 and series 2, which differ nominally only by the cap-layer-growth conditions. Clear differences between the diffraction profiles of the two samples are visible. In addition, Fig. 1 contains theoretical diffraction profiles calculated on the basis of dynamical-diffraction theory. The nearly perfect accordance between the measurements and simulations enables to extract the total CdSe content in the samples very accurately. The difference between the two experimental curves is caused by a clearly different amount of CdSe in the two samples. The total CdSe content for all samples of series 1 and 2 is presented in Fig. 2. The samples of series 2 contain only half of the CdSe, which is found in the samples of series 1 at the same CdSe deposit. Thermal CdSe desorption cannot explain this observation because CdSe does not desorb at temperatures up to 330 °C. This was verified by heating of samples with uncapped CdSe layers at temperatures of up to 360 °C for several minutes. In this control experiment, a ZnSe cap layer was deposited afterwards by conventional MBE and the amount of CdSe was determined by HRXRD. The CdSe desorption rate was only 0.0012 ML/s at 360 °C.

Figure 3 exemplary shows the HRTEM micrograph of a sample of series 2, which was evaluated by digital analysis

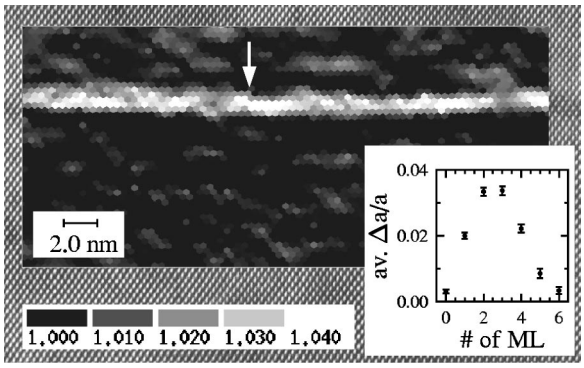

FIG. 3. HRTEM micrograph evaluated by DALI for 5 MEE cycles CdSe of series 2. The relative vertical lattice constant is gray scale coded. The inset shows the depth profile averaged from the arrow to the right side of the micrograph. The error bars give the statistical error. $\Delta a/a = 0.04$ corresponds to about 27% Cd using HRXRD for calibration.

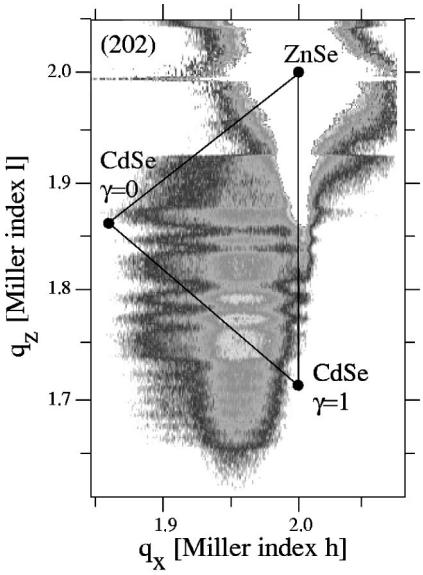

FIG. 4. Reciprocal space map for the (202) reflection of nominal 4.9-ML CdSe without cap layer measured by GIXRD. The intensity is gray-scale coded. The relaxation triangle of CdSe is given for comparison. A strain parameter $\gamma = 1$ corresponds to a pseudomorphic layer, $\gamma = 0$ to a fully relaxed layer.

of lattice images[5] (DALI). Compositional fluctuations can be seen that act as quantum dots.[13] A strong intermixing of CdSe and ZnSe and a rather symmetrical depth profile of the nominal binary CdSe layer are clearly visible, too. If this intermixing is caused by interdiffusion, it must occur partly already during the CdSe deposition because of the low CdSe growth rate of 0.029 ML/s. Thus the influence of interdiffusion was studied by GIXRD measurements on nominal 4.9-ML-thick CdSe without a ZnSe cap layer. Figure 4 presents a reciprocal space map for the (202) reflection. Using this reflection, strain and composition of the layers can be separated.[14] Dynamical calculations show that a simple kinematical evaluation is valid for this reflection. The signal of binary, partly relaxed CdSe is visible, which is superimposed by a modulation due to the finite size of the ZnSe buffer layer. The evaluation yields a strain parameter of $\gamma = 0.6$. This strong relaxation is attributed to the rather large CdSe thickness in case of this sample. The absence of intermixing before overgrowth is significant giving direct evidence for the importance of Cd surface segregation.

It was reported that the Cd sticking coefficient is strongly reduced if Zn and Cd are deposited at the same time under group-II-rich conditions.[15,16] The basic differences between MEE and conventional MBE are the very low growth rate and the deposition under alternately extremely group-II- and group-VI-rich conditions for MEE. Indeed, we find a similar CdSe reduction of about 33% by changing the VI/II flux ratio from group-VI- to group-II-rich conditions during CdSe overgrowth by MBE. This proves the importance of the VI/II flux ratio for the investigated process. Our experimental results can be explained by a segregation model, which takes into account partial redesorption of the Cd. During MEE, Cd atoms from the topmost surface layers are replaced by Zn atoms. Due to the smaller binding energy of Cd adatoms on

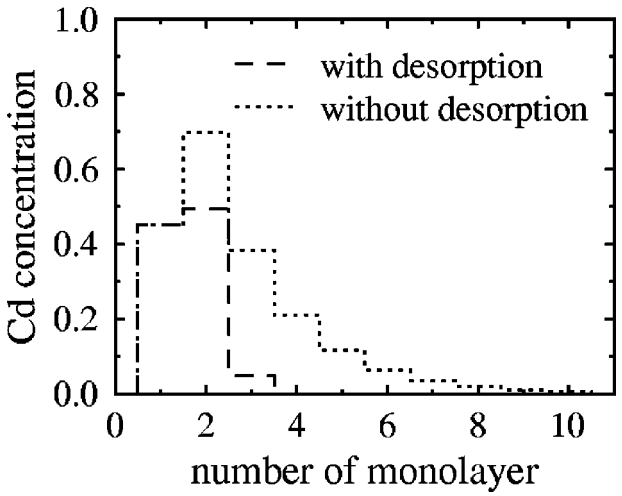

FIG. 5. Calculated composition profiles for nominal 2-ML CdSe, a segregation probability of 0.55, and a sticking probability of 0.18 (50% Cd desorption) and 1.00 (no Cd desorption).

ZnSe in comparison to Cd adatoms on CdSe, this process results in an effective redesorption of Cd that can be summarized as segregation-enhanced etching of Cd during Zn deposition. It should be mentioned that besides the top layer, some layers below also must be affected because the maximum CdSe loss would be 1 ML otherwise for all samples. Muraki *et al.*[17] proposed a model for the concentration dependence of the segregating element on the layer depth. Extending this model by a surface-desorption probability $(1-r)$ of the segregating element yields

$$x = x_0(1-R)\frac{1-(Rr)^n}{1-Rr}, \quad n \leqslant N,$$

$$x = x_0(1-R)\frac{1-(Rr)^N}{1-Rr}(Rr)^{n-N}, \quad n > N,$$

where x_0 is the nominal concentration, R is the segregation probability, N is the nominal number of deposited monolayers, and n is the number of the ongoing monolayer. In analogy to the model of Muraki *et al.*[17] it is assumed that R is independent of n. Although this assumption fails for x_0 approaching 1, it describes underlying atomic processes in a sufficient approximation even for thin quantum dot layers as shown below.

In our experiments, we observe the redesorption of half of the deposited Cd. Within our model this can be reproduced by various combinations of the segregation probability R and the desorption probability $(1-r)$ independent of the nominal CdSe thickness N. Nevertheless, a minimal segregation probability is implied, which is 0.5 for a total of 50% Cd loss. An upper limit of $R=0.6$ results from a comparison of the calculated composition profiles with the profiles determined by DALI, keeping in mind the errors of DALI. Thus a segregation probability of $R=0.5$–0.6 can be extracted. Figure 5 exemplarily shows the calculated depth profiles obtained for $N=2$, $R=0.55$, and $r=0.18$ (50% Cd loss) or $r=1.00$ (no Cd loss), respectively. The concentration profile for $r=0.18$ is nearly symmetrical. Thus we like to point out that nearly symmetrical concentration profiles do not necessarily rule out the presence of surface segregation during growth.

The calculated concentration profiles assuming $R=0.55$ and $r=0.18$ are narrower than the depth profiles obtained by DALI (see inset of Fig. 3), but the averaging of the HRTEM over the specimen thickness has to be taken into account for a detailed comparison. Due to this averaging, a monolayer roughness of interfaces results in an apparent broadening of the CdSe film. Secondly, Cd interdiffusion can cause an additional broadening of the experimental concentration profiles. If interface roughness is neglected for the moment, the determined diffusion constants are 2×10^{-19}cm^2/s–1.8×10^{-18}cm^2/s for the samples of series 2. As the samples were prepared under experimentally identical conditions, such large differences in the diffusion constant are unlikely. Hence these differences must be attributed to a strong variety in the interface roughness in different HRTEM samples. Thus 2×10^{-19} cm^2/s is the upper limit for a diffusion constant which is in accordance with our experimental results.

Rosenauer *et al.*[5] reported a composition profile for a CdSe film grown at 300 °C corresponding to a segregation probability $R=0.6$. Peranio *et al.*[11] published a mean segregation probability $R=0.55$ for samples grown at 280 °C. Both values are comparable with that of this work. This agreement is surprising due to the low growth rate of MEE. However, our upper limit for the diffusion constant is three orders of magnitude lower than that reported by Peranio *et al.*[11] The maximum value for the diffusion constant, as extrapolated to growth temperature from annealing experiments for undoped samples,[5,18,19] is of the order of 10^{-20}cm^2/s. Thus it is only one order of magnitude smaller than our result. The remaining difference can be explained by the presence of interface roughness (indicated by the arrow in Fig. 3), which is neglected in our analysis.

In conclusion, we find a Cd redesorption of 50% if the ZnSe cap layer was grown by MEE compared to MBE. This could be quantitatively explained by a segregation model, which takes into account a partial redesorption of segregating Cd atoms. The underlying process can be summarized as segregation-enhanced etching of Cd during Zn deposition. The used model leads to nearly symmetrical composition profiles pointing to the fact that such profiles are not necessarily caused by interdiffusion. We demonstrated that no intermixing occurs before overgrowth for the samples under study, indicating the importance of surface segregation in CdSe/ZnSe quantum-dot structures. The presented experimental results give evidence that the growth conditions during overgrowth of the CdSe by ZnSe are of particular importance when discussing the intermixing process of CdSe and ZnSe. This proves that Cd interdiffusion is not the main cause for intermixing under common growth conditions.

The authors are grateful to A. Rosenauer and D. Gerthsen for providing the DALI software. This work was supported by the Deutsche Forschungsgemeinschaft.

*Electronic address: tpassow@physik.uni-bremen.de

[1] F. Flack, N. Samarth, V. Nikitin, P. A. Crowell, J. Shi, J. Levy, and D. D. Awschalom, Phys. Rev. B **54**, R11 074 (1996).
[2] S. H. Xin, P. D. Wang, Yin Aie, C. Kim, M. Dobrowolska, J. L. Merz, and J. K. Furdyna, Appl. Phys. Lett. **69**, 3884 (1996).
[3] M. Rabe, M. Lowisch, and F. Henneberger, J. Cryst. Growth **184/185**, 248 (1998).
[4] K. Leonardi, H. Selke, H. Heinke, K. Ohkawa, D. Hommel, F. Gindele, and U. Woggon, J. Cryst. Growth **184/185**, 259 (1998).
[5] A. Rosenauer, T. Reisinger, E. Steinkirchner, J. Zweck, and W. Gebhardt, J. Cryst. Growth **152**, 42 (1995).
[6] M. Strassburg, V. Kutzer, U. W. Pohl, A. Hoffmann, I. Broser, N. N. Ledentsov, D. Bimberg, A. Rosenauer, U. Fischer, D. Gerthsen, I. L. Krestnikov, M. V. Maximov, P. S. Kop'ev, and Zh. I. Alferov, Appl. Phys. Lett. **72**, 942 (1998).
[7] T. Passow, K. Leonardi, A. Stockmann, H. Selke, H. Heinke, and D. Hommel, J. Phys. D **32**, A42 (1999).
[8] R. N. Kyutt, A. A. Toropov, S. V. Sorokin, T. V. Shubina, S. V. Ivanov, M. Karlsteen, and M. Willander, Appl. Phys. Lett. **75**, 373 (1999).
[9] H. Heinke, T. Passow, A. Stockmann, H. Selke, K. Leonardi, and D. Hommel, J. Cryst. Growth **214/215**, 585 (2000).
[10] E. Kurtz, M. Schmidt, M. Baldauf, S. Wachter, M. Grün, D. Litvinov, S. K. Hong, J. X. Shen, T. Yao, D. Gerthsen, H. Kalt, and C. Klingshirn, J. Cryst. Growth **214/215**, 712 (2000).
[11] N. Peranio, A. Rosenauer, D. Gerthsen, S. V. Sorokin, I. V. Sedova, and S. V. Ivanov, Phys. Rev. B **61**, 16 015 (2000).
[12] A. Rosenauer, W. Oberst, D. Litvinov, D. Gerthsen, A. Förster, and R. Schmidt, Phys. Rev. B **61**, 8276 (2000).
[13] F. Gindele, U. Woggon, W. Langbein, J. M. Hvam, K. Leonardi, D. Hommel, and H. Selke, Phys. Rev. B **60**, 8773 (1999).
[14] K. Zhang, Ch. Heyn, W. Hansen, Th. Schmidt, and J. Falta, Appl. Phys. Lett. **77**, 1295 (2000).
[15] T. Seedorf, M. Cornelissen, K. Leonardi, D. Hommel, H. Selke, and P. L. Ryder, J. Cryst. Growth **214/215**, 602 (2000).
[16] S. Ivanov, S. Sorokin, I. Krestnikov, N. Fleev, B. Ber, I. Sedova, Yu. Kudryavtsev, and P. Kop'ev, J. Cryst. Growth **184/185**, 70 (1998).
[17] K. Muraki, S. Fukatsu, Y. Shiraki, and R. Ito, Appl. Phys. Lett. **61**, 557 (1992).
[18] M. K. Chai, S. F. Wee, K. P. Homewood, W. P. Gillin, T. Cloitre, and R. L. Aulombard, Appl. Phys. Lett. **69**, 1579 (1996).
[19] M. Kuttler, M. Strassburg, O. Stier, U. W. Pohl, D. Bimberg, E. Kurtz, J. Nürnberger, G. Landwehr, M. Behringer, and D. Hommel, Appl. Phys. Lett. **71**, 243 (1997).